Aluminum in liver cells - the element species matters

Holger Sieg, Anna Lena Ellermann, Birgitta Maria Kunz, Pégah Jalili, Agnès Burel, Kevin Hogeveen, Linda Böhmert, Soizic Chevance, Albert Braeuning, Fabienne Gauffre, et al.

Aluminum in liver cells – The element species matters

Holger Sieg[1], Anna Lena Ellermann[1], Birgitta Maria Kunz[1], Pégah Jalili[2], Agnès Burel[3], Kevin Hogeveen[2,5], Linda Böhmert[1], Soizic Chevance[4], Albert Braeuning[1], Fabienne Gauffre[4], Valérie Fessard[2] and Alfonso Lampen[1]

[1] German Federal Institute for Risk Assessment, Dept. Food Safety, Max-Dohrn-Straße 8-10, 10589 Berlin

[2] ANSES, French Agency for Food, Environmental and Occupational Health Safety, Fougères Laboratory, 10B rue Claude Bourgelat, 35306, Fougères Cedex, France

[3] Univ Rennes, Biosit - UMS CNRS 3480 - INSERM 018, F-35000 Rennes, France

[4] Univ Rennes, CNRS, ISCR (Institut des Sciences Chimiques de Rennes) - UMR 6226, F-35000 Rennes, France

[5] ASPIC Cellular Imaging Platform, 10 B rue Claude Bourgelat, 35306 Fougères, France

Corresponding Author:

Holger Sieg, holger.sieg@bfr.bund.de

Keywords

Nanoparticles, Aluminum, Toxicology, Liver, HepG2, HepaRG, Oxidative Stress, Apoptosis

Abstract

Aluminum (Al) can be ingested from food and released from packaging and can reach key organs involved in human metabolism, including the liver via systemic distribution. Recent studies discuss the occurrence of chemically distinct Al-species and their interconversion by contact with biological fluids. These Al species can vary with regard to their intestinal uptake, systemic transport and therefore could have species-specific effects on different organs and tissues. This work aims to assess the *in vitro* hepatotoxic hazard potential of three different relevant Al species: soluble $AlCl_3$ and two nanoparticulate Al species were applied, representing for the first time an investigation of metallic nanoparticles besides to mineral bound γ-Al_2O_3 on hepatic cell lines.

To investigate the uptake and toxicological properties of the Al species, we used two different human hepatic cell lines: HepG2 and differentiated HepaRG cells. Cellular uptake was determined by different methods including light microscopy, transmission electron microscopy, side-scatter analysis and elemental analysis. Oxidative stress, mitochondrial dysfunction, cell death mechanisms and DNA damage were monitored as cellular parameters.

While cellular uptake into hepatic cell lines occurred predominantly in the particle form, only ionic $AlCl_3$ caused cellular effects. Since it is known, that Al species can convert one into another, and mechanisms including “trojan-horse”-like uptake can lead to an Al accumulation in the cells. This could result in the slow release of Al ions, for which reason further hazard cannot be excluded. Therefore, individual investigation of the different Al species is necessary to assess the toxicological potential of Al particles.

Introduction

Aluminum (Al) is one of the most frequent elements and is mainy found bound in minerals. It can dissolve, promoted by natural and industrial processes, and is also industrially produced in its metallic form (Exley, 2003, Wagner, 1999, Emsley, 1991, Lote and Saunders, 1991). Various Al species are used for multiple applications, including food and food contact materials, what leads to human exposition via several uptake routes (Willhite et al., 2012, Schintu et al., 2000, Stahl et al., 2011, Echegoyen et al., 2016). A fraction of 0.1 – 5 % of ingested Al obtains systemic bioavailability (Van Oostdam et al., 1990, Yokel et al., 2005, Krewski et al., 2007, Schönholzer et al., 1997) and gets deposited in organs, mostly in bones, lungs, muscles, liver and brain (Krewski et al., 2007). In general, Al reaches hepatic concentrations between 1 and 2.45 mg/kg liver weight and accumulates over the human lifetime (Nieboer et al., 1995, Caroli et al., 1994, Keith et al., 2002). Al accumulation can be much higher in patients suffering from renal insufficiency, where hepatic Al concentrations above 300 mg/kg organ weight were measured (Alfrey et al., 1980). Organ burden of Aluminum has been reviewed in detail (Krewski et al., 2007).

Physicochemical characteristics of Al, such as particle size distribution, ion release and surface coating can be changed when getting in contact with gastrointestinal fluids (Sieg et al., 2017). These changes were analyzed detailed with a variety of analytical techniques. During the passage of the GI-tract, there occurs not only dissolution but also agglomeration / aggregation as well as particle formation from soluble Al species. The quantity of uptake and transport across the gastrointestinal barrier (of around 0.1 to 5 %) depends on the respective Al species (Sieg et al., 2018). This could result in a variety of particle- and ion-specific effects which need to be considered.

The hazard potential of Al is still unclear (Willhite et al., 2014, Lidsky, 2014) although the oral Al exposition in humans is known to be close to the TWI of 1 mg/kg BW/week. While links to blood and bone diseases have been documented (Alfrey et al., 1976, Vick and Johnson, 1985, Lin et al., 2013), the role of Al in breast cancer and neurodegenerative disorders is still disputed (Darbre, 2009, Walton, 2014). In animal studies, Al treatment showed hepatotoxic outcomes (Ghorbel et al., 2016). In general, these toxic effects have been attributed to oxidative stress (Abdel-Wahab, 2012, Yuan et al., 2012), mitochondrial dysfunction (Swegert et al., 1999, Xu et al., 2017), or DNA damage (Kumar et al., 2009). Lipid peroxidation was also observed (Zatta et al., 2002). Most of these studies investigated soluble Al in form of citrate, chloride or other salts. However, contradictory effects have been published for Al_2O_3 nanoparticles (Chen et al., 2008, Zhang et al., 2011, Radziun et al., 2011, Sun et al., 2011), while elementary Al nanoparticles have not been investigated with this focus before. This

study aims to investigate Al species-specific cellular uptake and molecular effects of Al in two frequently used human hepatic cell lines, HepG2 and HepaRG. Both cell lines are widely used models with different advantages and applicability: HepG2 are a quick and easy to handle standard hepatoma model (Gerets et al., 2012), while HepaRG culture is more complex and time-consuming while being closer to normal hepatocyte physiology, especially with respect to liver cell metabolism (Aninat et al., 2006, Antherieu et al., 2010). Both models were used in parallel to get a more representative impression on the effects on liver cells, and a variety of analytical and toxicological *in vitro* methods was applied.

Materials and Methods

Chemicals and nanoparticles

Standard chemicals were purchased from Sigma-Aldrich (Taufkirchen, Germany), Merck (Darmstadt, Germany), or Carl Roth (Karlsruhe, Germany) in the highest available purity. Nanomaterials (Al^0-core surface-passivated nanoparticles and γ-Al_2O_3 nanoparticles) were supplied by IoLiTec (Heilbronn, Germany). Al^0 nanoparticles were stored and weighed under an argon atmosphere. Both particles were freshly dispersed according to the modified NanoGenoTOX protocol (ultrasonication with KE76 for 5'09'' with ~20% energy), stabilized by 0.05% BSA/water before use (Krause et al., 2018). BSA was supplied by Carl Roth (Albumin Fraction V, ≥98%) and $AlCl_3$ was supplied by Sigma-Aldrich (Hexahydrate, ≥97%).

Light and transmission electron microscopy

Cell imaging was performed with the light microscope Zeiss Axio Observer D1/5 with AxioCAM MR R3 using a magnification of 200 fold and ZEN lite 2012 software. For transmission electron microscopy (TEM), after 24 h exposure to nanoparticles, HepaRG cells were rinsed with 0.15 M Na cacodylate buffer (Sigma Aldrich) and fixed by drop-wise addition of glutaraldehyde (2.5%) for 1 h. After fixation, the specimens were rinsed several times with 0.15 M Na cacodylate buffer and postfixed with 1.5% osmium tetroxide for 1 h. After further rinsing with cacodylate buffer, the samples were dehydrated through a series of graded ethanol from 70 to 100%. The specimens were infiltrated in a mixture of acetone–eponate (Sigma Aldrich) (50/50) for 3 h and then in pure Eponate for 16 h. Finally, the specimens were embedded in DMP30–Eponate for 24 h at 60 °C. Sections (0.5 µm) were cut on a Leica UC7 microtome and stained with toluidine blue. Ultrathin sections (90 nm) were obtained, collected onto copper grids, and counterstained with 4% uranyl acetate (Serva, Heidelberg, Germany) and then with lead citrate (Sigma Aldrich). Examination was performed with a

JEOL 1400 transmission electron microscope operated at 120 kV equipped with a 2k-2k camera from Gatan (Orius 1000).

Cell cultivation

HepG2 cells (ECACC 85011430, Porton Down, UK) were cultivated in DMEM High Glucose, 10 % fetal calf serum (FCS), and 100 U/mL penicillin 100 µg/mL streptomycin (GE Healthcare, Solingen, Germany). Cells were seeded into each well of cell culture plates (20,000 cells per 96-well, 220,000 cells per 12-well to guarantee equal cell density in the different culture formats) and used for experiments 24 h after seeding. HepaRG cells (Biopredic HPR101, St. Gregoire, France) were cultivated according to the recommended protocol (Luckert et al., 2017) using William's E Medium (PAN-Biotech, Aidenbach, Germany) supplemented with 10 % (v/v) fetal calf serum, 100 U/mL penicillin and 100 µg/mL streptomycin, 5 µg/mL insulin (PAA Laboratories GmbH, Pasching, Austria) and 5×10^{-5} M hydrocortisone hemisuccinate (Sigma-Aldrich, Taufkirchen, Germany). Cells were cultivated for 2 weeks without supplementing DMSO and for another 2 weeks with supplementing up to 1.7 % DMSO, changing the medium every 2 – 3 days. Particle dispersions were diluted freshly prior to use into serum-containing cell culture medium to adjust the desired concentrations and regular growth conditions. The cellular medium supernatant was then removed and the cells incubated with the prepared solutions for 24 or 48 h. In previous studies, particle stability in cell culture medie under incubation conditions was confirmed using analytical techniques like small-angle x-ray scattering (SAXS) or dynamic light scattering (DLS) (Sieg et al., 2018, Krause et al., 2018).

Element Analysis / AAS

Cellular uptake of Al species was determined by Atomic Absorption Spectroscopy (AAS). Cells were incubated with 50 µg of the different Al species in 1 mL medium for 24 h in 12-well plates. After incubation, the medium was collected and cells were washed twice with 500 µL PBS to remove loosely bound extracellular particles. Cells were harvested by scraping in 500 µL deionized water and collected in a microwave digestion tube. Acidic hydrolysis was performed (69 % HNO_3, 180 °C for 20 min in an MLS-ETHOS Microwave system) followed by element analysis with AAS (Perkin Elmer AAnalyst 800, Shelton, USA) as in previous studies (Lichtenstein et al., 2016). The absorbed amount of Al (50 µg initially administered Al mass) is shown as mean values of at least 6 replicates with standard deviations.

Cytotoxicity assays and cellular effects

Cell viability was measured by the Cell Titer Blue assay (CTB; Promega, WI USA) followed by the MTT assay. The cells were incubated in a volume of 100 µL for 24 h or 48 h in 96-well-plates. After the incubation time, 20 µL CTB reagent (Promega, 1:4 in PBS) were added. After further 30 to 60 min, fluorescence was measured with a Tecan plate reader (Ex. 560, Em. 590 nm). Subsequently, 10 µL of 5 mg/mL 3-(4,5-Dimethylthiazol-2-yl)-2,5-diphenyltetrazolium bromide (Sigma Aldrich, MTT) in PBS was added for another hour. Afterwards, media were removed and 130 µL desorption agent (0.7 % w/v SDS in isopropanol, Roth, Germany) was added. Plates were shaken for 30 min and absorption was measured with a plate reader (570 nm) while background absorption (630 nm) was subtracted. Results are given normalized to untreated controls, after subtraction of equally treated cell-free reference wells. The neutral red uptake assay (NRU) was performed according to the previously described protocol (Repetto et al., 2008). Triton X-100 (0.01 %) was used as a positive control. Statistics were performed as Student's t-test indicated by asterisks (* $p<0.05$; ** $p<0.01$; *** $p<0.001$).

Cellular impedance was determined by an xCELLigence system (Roche, Basel, Switzerland). Cells were seeded and differentiated (for HepaRG) in gold-coated 96-well E-plates and incubated with 100 µL of the testing substances or controls, and measured over a time period of 48 h. The cell index was calculated as mean values of at least 3 replicates with standard deviation. Cell indices were normalized twice, on time point 0 and untreated controls. As a cytotoxic positive control, ZnO particles (IoLiTec, Heilbronn, Germany) were used.

Cellular effects were determined in 96-well plates. To measure reduced GSH levels, we used the previously published monochlorobimane assay (Kamencic et al., 2000). After incubation with the test substances, media were removed and 250 µL PBS with 40 µM monochlorobimane (MCB, Sigma Aldrich) was added into each well for 20 to 30 min. Afterwards, cells were washed with 250 µL PBS, incubated with 150 µL desorption agent (see above), and shaken for 30 min. Fluorescence was measured with a plate reader (Ex. 380 nm, Em. 460 nm). Mean values were determined as described. 100 µM buthioninesulfoximine (BSO, Sigma Aldrich) was used as a positive control for GSH-level reduction.

Mitochondrial depolarization was determined by the JC1 assay. After incubation, samples were removed and 100 µL of a 1 mg/mL JC1 solution (Santa Cruz, Dallas, USA) in PBS was added for 20 min. Cells were washed twice with 250 µL PBS and finally 100 µL PBS was added for fluorescence measurements. Fluorescence was measured (green: Ex: 485 nm, Em. 535 nm; red: Ex: 535 nm, Em. 595 nm), the red/green fluorescence ratio was determined, and mean values were normalized on untreated controls. As a positive control

for mitochondrial depolarization, 1 mg/mL valinomycine (Thermo Fisher Scientific, Whatman, USA) was used and added 2 h before the end of incubation time.

Flow cytometric assays

Apoptosis / necrosis measurements and cell cycle analysis were performed by flow cytometry using a BD Accuri C6 (Accuri, Belgium). HepaRG cells were cultivated and incubated as described before, HepG2 cells were grown in 12-well plates. After incubation, cells were washed with PBS, harvested with trypsin/EDTA, and collected in serum-containing cell culture medium. All supernatants of each sample were pooled and centrifuged (3 min, 200 x g) to collect the cells. Cells were washed with cold PBS and annexin buffer (5 mM Hepes, 70 mM NaCl, 2.5 mM $CaCl_2$, pH 7.4). For staining, AnnexinV-FITC and 7AAD (ImmunoTools, Oldenburg, Germany), were mixed with annexin buffer in the ratios 1:20 and 1:10. The cells were stained for 30 min in the solution and measured by the flow cytometer to a maximum of 10,000 cells per sample. Fluorescence was detected for FITC (Ex: 488, Em: 533/30 nm) and 7AAD (Ex: 488 nm, Em: >670 nm). Color compensation was performed to avoid interactions between both fluorophores. The background level was determined by untreated stained controls. AxV-positive were defined as apoptotic and 7AAD-positive or double-positive cells were defined as late-apoptotic / necrotic. Relative cell numbers of the populations were averaged from at least two independent experiments with at least three replicates each condition; error bars show standard deviations. Statistics were performed by Student's t-test indicated by asterisks (* $p<0.05$; ** $p<0.01$; *** $p<0.001$). As positive controls, 2 µM staurosporine for apoptosis (Santa Cruz) and 50 µM *tert*-butyl hydroxyperoxide (tBOOH) for necrosis (Sigma Aldrich) were used. In the same experiment, side scatter was determined among the selected viable cells. Cells were defined as "highly granular", if their side scatter was higher than the 97th percentile of the control cells.

High Content Analysis

After a 24 h treatment with test compounds, cells were fixed for 10 min with 4 % formaldehyde in PBS and permeabilized with 0.2 % Triton X-100. Following three washing steps with PBS-Tween 0.05 %, plates were incubated in blocking solution (PBS with 1 % BSA and 0.05 % Tween-20) for 30 min before addition of primary antibodies. Anti ATM pS1981 (ab19304) and anti γH2AX ser139 (ab26350) were purchased from Abcam (Cambridge, UK), anti p53 pS15 was purchased from Thermo Fisher Scientific (Villebon-sur-Yvette, France). All antibodies were prepared in blocking solution. Primary antibodies were incubated overnight at 4°C. After washing with PBS + 0.05% Tween-20, secondary antibodies (goat anti-mouse IgG AlexaFluor 647 (ab150115), goat anti-rabbit IgG AlexaFluor

555 (ab150078) (Abcam, Cambridge, UK) were incubated for 45 min at room temperature. Nuclei were stained with DAPI (1 µg/mL in PBS) for 5 min for automated cell identification by high content analysis.

Plates were scanned using an ArrayScan VTI HCS Reader (Thermo Scientific, Waltham, USA) and were analyzed using the Target Activation module of the BioApplication software. For each well, 5 fields (10× magnification) were scanned and analyzed for quantification of immunofluorescence. Cytotoxicity was determined by cell counts from DAPI staining and was expressed as percentage of cells compared to control cells. γH2AX, ATM and p53 were quantified in cell nuclei and expressed as fold increases relative to control cells. At least three independent experiments were performed.

Statistical Analysis

Statistical analysis occured using Student's t-test comparing the mean values of all biological replicates to untreated controls. For High-Content-Analysis, recommended median values were used. Error bars indicate standard deviations. Statistical significance is indicated by asterisks (* $p<0.05$; ** $p<0.01$; *** $p<0.001$).

Results

All experiments were performed with two human *in vitro* liver cell models, HepG2 and HepaRG. These cell models were treated with 3 representative Al-species: Elementary, metallic Al^0 nanoparticles, Al_2O_3 nanoparticles and soluble $AlCl_3$. The particle characterization was published before (Sieg et al., 2017, Sieg et al., 2018, Krause et al., 2018)and is listed in Supplementary Table 1. The cellular uptake of the different Al species into both cell lines was investigated by four different methods: light microscopy, side scatter analysis, element analysis and TEM (Figure 1).

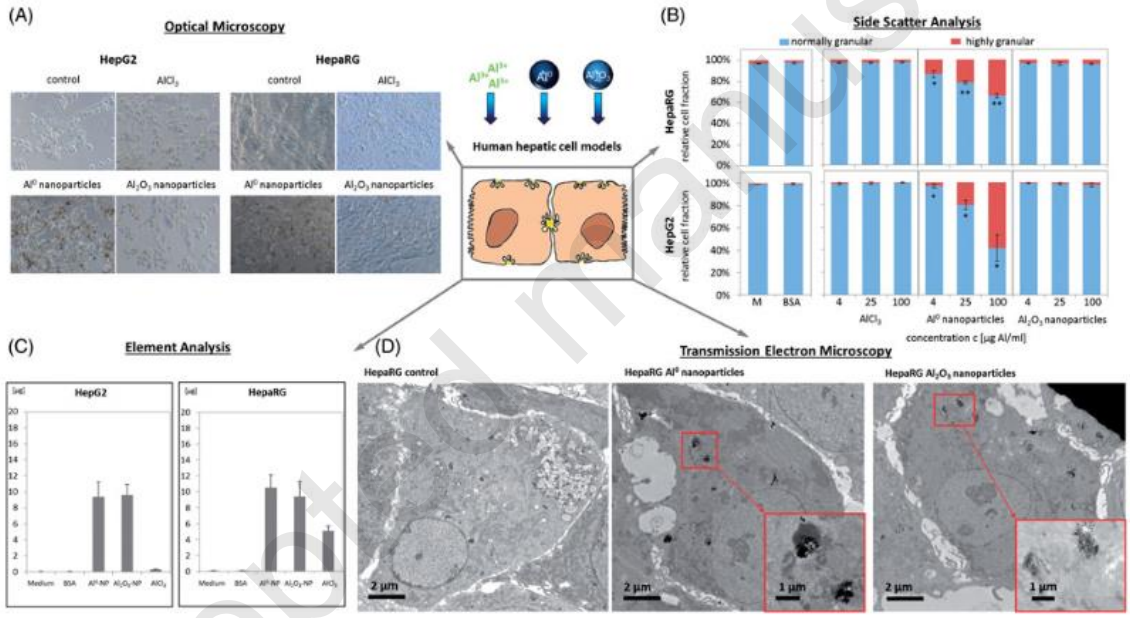

Figure 1: Cellular uptake of Al into liver cells. A: Light microscopy. HepG2 (left) and HepaRG (right) were incubated with 50 µg Al/mL of the different Al species and controls for 24 h and visualized by optical microscopy at 200-fold magnification. B: Side scatter analysis was performed by flow cytometry after 24 h of incubation of HepG2 and HepaRG cells with the Al species followed by annexin-V/7AAD staining. The threshold for "highly granular" cells was defined as cells with a side scatter higher than the 97th percentile of untreated control cells. 10.000 cells were counted per sample and the experiments were done in at least 3 replicates for each condition. Statistical significance was determined by Student's t-test and is indicated by asterisks (* p<0.05; ** p<0.01). C: Aluminum quantification performed by element analysis after incubation of HepG2 and HepaRG cells with 50 µg Al/mL Al-species and controls for 24 h followed by washing, cell harvesting, microwave HNO_3 digestion and AAS measurement. The experiment was done in 6 replicates and samples were measured at least 4 times. D: For TEM , HepaRG cells were

treated with 19 µg/mL Al^0 and Al_2O_3 nanoparticles. After 24 h, controls and treated cells were analyzed using electron microscopy to detect particle uptake. Enlarged pictures can be found in Supplementary Figure 1.

All four methods indicated uptake of Al into liver cells. For a first impression, cells were observed by light microscopy (Figure 1A). Both cell lines revealed observable dark discolorations in the cytoplasm especially for the gray-metallic Al^0 nanoparticles. Although it is not possible to discriminate between uptake and external interaction by light microscopy, the pictures show particle aggregation associated to the cells, likely inside the cytoplasm. There were no significant differences observed between the HepG2 cell clusters and the monolayer of differentiated HepaRG cells. Ionic $AlCl_3$ as well as Al_2O_3 nanoparticles were less visible in the microscope. To confirm cellular uptake of Al^0 and Al_2O_3 nanoparticles, TEM was used by examination of cell cross-sections, which show particle agglomerates in the cytoplasm (Figure 1D). This uptake was especially pronounced for Al_2O_3 species with dark agglomerates. Al particles were localized in the cytoplasm in dark compartments like lysosomes, there is no nucleus entrance. The ion Al uptake was not possible to analyze by TEM, because particles formed *de novo* from ionic Al can be easily confused with contrasted cytoplasmic components and are very difficult to identify in complex matrices. As another method, side scatter analysis was performed to determine the cell fraction that had taken up Al nanoparticles after 24 h incubation time (Figure 1B). The dose-dependent increase of cell granularity indicated cellular uptake of Al^0 nanoparticles (up to 50 % positive cells) into both cell lines, supporting the microscopy results. A majority of HepG2 cells had taken up these particles, whereas the cellular fraction of HepaRG cells which internalized Al^0 nanoparticles was slightly lower. Side scatter analysis is only applicable for particles with a strong light scattering character. For this reason, there were no obvious effects detected for the both other Al species. Element analysis via AAS allows the investigation of ionic species and low-refractive particle species as well. Both cell lines have taken up Al from the particulate Al species in almost equal amounts (Figure 1C). The absorbed fraction accounted for 18 to 22 % of the administred Al, respectively, regardless to the cell line and the morphological properties of the cells and the types of particles. Surprisingly, there were big differences between both cell lines regarding the uptake of ionic $AlCl_3$.

Since it could be shown that the observed Al species can be taken up by hepatic cells, we investigated the impact of these Al species on the cell viability and cellular responses.

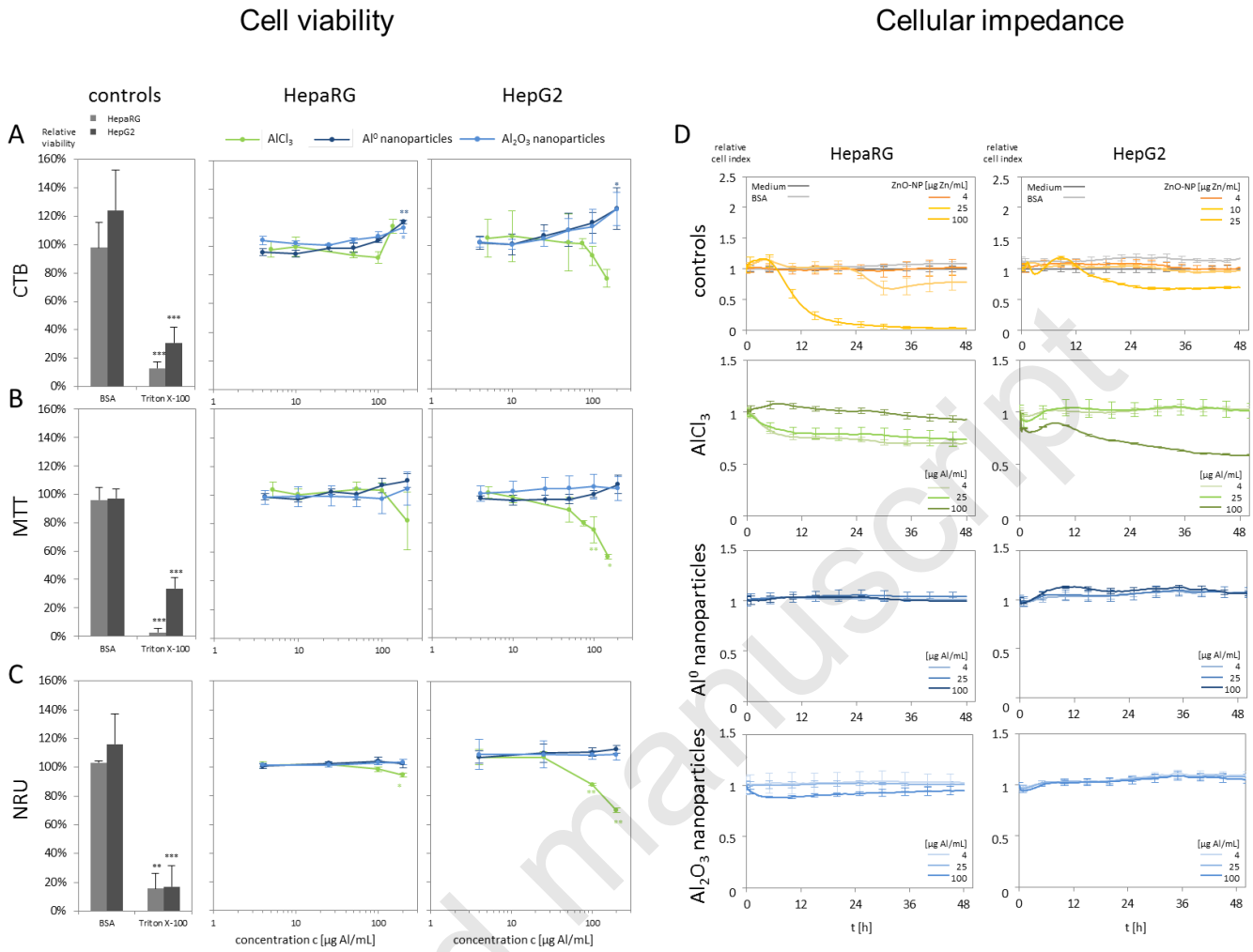

Figure 2: Cell viability measurement by three different methods: CTB (A), MTT (B), and NRU (C) after 48 h incubation with Al species. 0.01 % Triton X-100 was used as positive control for cytotoxicity. Results were normalized to medium control and are given as mean values and standard deviations of at least 3 independent experiments. Statistical significance was determined by Student's t-test and is indicated by asterisks (* p<0.05; ** p<0.01; *** p<0.001). (D) Measurement of cellular impedance by xCELLigence technology after incubation with Al species over a time period of 48 h. Relative cell indices were normalized to the initial cell index and the medium control. Mean values calculated from at least 3 replicates are given together with the respective standard deviations. 100 µg Zn/ml ZnO nanoparticles (IoLiTec) were used as toxic positive control.

To determine species-specific acute toxic effects of Al, three different cell viability assays were performed (Figure 2A-C). With regard to all three testing systems, no acute cytotoxicity was measurable for the particulate Al species. In contrast, high concentrations of $AlCl_3$ of 100 µg Al/mL (894 µg $AlCl_3$/mL) or more showed toxic effects mainly on HepG2 cells. This cell line tended to be more sensitive to Al than HepaRG. Only the highest concentration of $AlCl_3$ (200 µg Al/mL) had a minimal, but a statistically significant toxic effect on HepaRG cells in the NRU test. These high concentrations of $AlCl_3$ on HepaRG cells, however, led to strong interactions with the testing system in the CTB and MTT assay and therefore could not be

taken into account. Even though the cellular uptake of Al from Al-containing nanoparticles was higher, the impact on cell viability was triggered by the ionic Al species. In addition, cell indices were determined as a surrogate for changes in the cellular impedance (Figure 2D). Consistently with the cytotoxicity measurements, cellular impedance was only impaired at high concentrations (100 µg Al/mL) of ionic Al. Effects were shown on both cell lines: HepG2 data indicated cell death over the observed time of 48 h, while HepaRG cells showed indications for changes in the cell monolayer rather than for cell death. In HepaRG, no time-dependent decrease of the relative cell indices was observed, in contrast to the HepG2 cells or positive controls.

Cellular effects can be caused by different mechanisms and particle uptake was previously described to be in relation to for example oxidative stress (Sieg et al., 2018). Therefore, we investigated several cellular endpoints to further characterize mechanisms of toxicity which can be caused by the Al species.

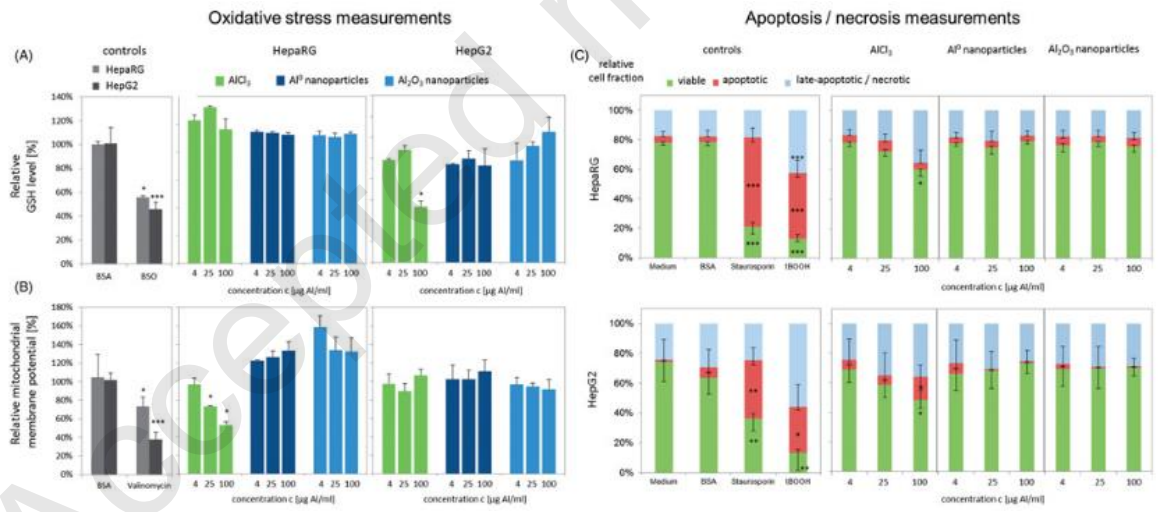

Figure 3: Measurement of cellular endpoints after 24 h incubation of HepG2 and HepaRG cells with Al species and controls. (A) Determination of relative GSH levels by monochlorobimane assay. (B) Relative mitochondrial membrane potential determined by JC1 assay. 100 µM BSO (A) and 1 mg/mL valinomycin (B) were used as positive controls. Values are presented as the mean percentage with standard deviation (n ≥ 3), normalized to medium control. Statistical significance was determined by Student's t-test and is indicated by asterisks (* p<0.05; ** p<0.01; *** p<0.001). (C) Apoptosis/necrosis measurements by flow cytometry after AxV/7AAD staining. As positive controls, 2 µM staurosporine and 50 mM *tert*-butyl hydroxyperoxide were used.

The further observed cellular endpoints, shown in Figure 3, included oxidative stress, mitochondrial function, and cell death (apoptosis / necrosis). Oxidative stress was analyzed via monitoring of the levels of reduced glutathione (GSH) .Mitochondrial depolarization was shown by the JC1 assay. Apoptosis and necrosis were quantified using AxV/7AAD staining and flow cytometry. Similar to previous experiments, both particle species had no influence on any cellular endpoint, while there were differences in the impact of ionic Al on the two cell lines: in HepG2 cells, a clear reduction of GSH indicated oxidative stress. No GSH reduction, however, was measurable in HepaRG cells, but a concentration-dependent reduction of mitochondrial membrane potential was observable in these cells, which is also a measure for oxidative stress. Both cell lines showed indications for reduced cell viability and apoptosis after $AlCl_3$ treatment. HepG2 cells tended again to be more sensitive to Al than HepaRG cells.

To observe possible genotoxic effects, high content analysis of both cell lines was performed (Figure 4). All three observed genotoxic endpoints (phospho-ATM, phospho-p53 and γH2AX) revealed no indication of DNA damage. In HepG2 cells, there was a slight decrease of signals after incubation with 100 µg Al/mL of the ionic species, probably as a result of the associated cytotoxicity. The experiments were nevertheless meaningful, illustrated by MMS which led to increased signals of all markers in both cell lines.

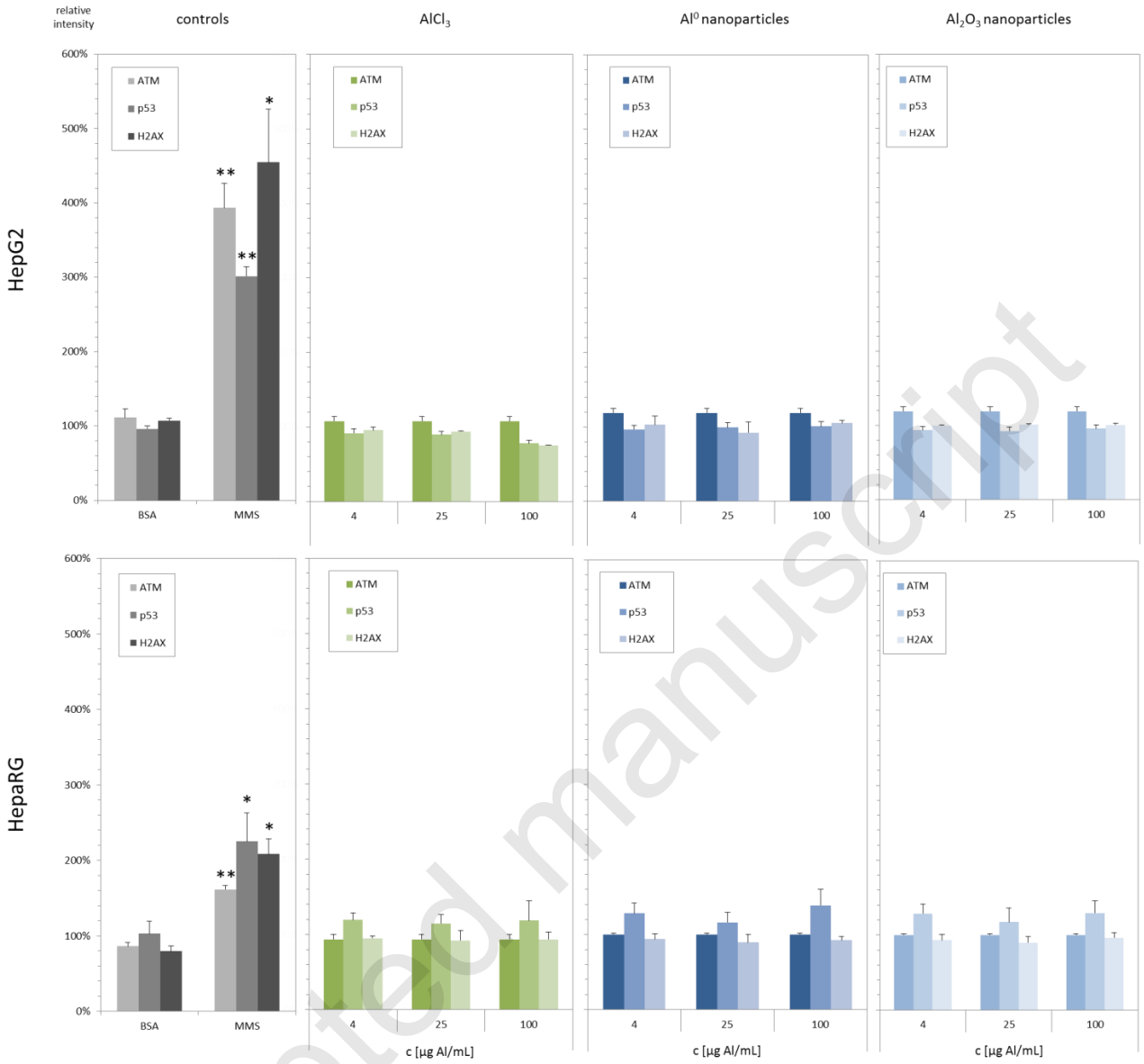

Figure 4: Determination of DNA damage in HepG2 and HepaRG cells after 24 h incubation with Al species and controls. Phospho-ATM, phospho-p53 and γH2AX were quantified in the nuclei of treated by High Content Analysis using an Arrayscan VTi automated microscope for genotoxicity markers. Experiments were performed in 3 replicates per condition and repeated 3 times in independent experiments. As positive control for DNA damage, 50 µg/mL MMS was used. Statistical significance was determined by Student's t-test and is indicated by asterisks (* p<0.05; ** p<0.01; *** p<0.001).

Discussion

Previous studies have demonstrated that up to 5 % of orally absorbed Al can pass the gastrointestinal barrier and obtains systemic bioavailability following oral exposure (Cunat et al., 2000). About 2 % of systemic Al is excreted via biliary fluids secreted by the liver (Willhite et al., 2014), and over the lifetime, an accumulation of Al occurs in the liver (Keith et al., 2002) reaching levels of 1 to 2.45 mg Al/kg liver (Caroli et al., 1994). Liver cells in *in vitro* cultures are directly exposed to Al without being protected by the gastrointestinal barrier. Previous experiments with the same nanoparticles and testing conditions on intestinal cells showed lower Al uptake of only 1 to 3 % of the administered (Sieg et al., 2018), as compared to up to 20 % in this study on liver cell lines, which were exposed to 50 µg Al for 24 h. Cellular uptake under *in vitro* conditions needs to be interpreted with care. *In vitro* intestinal cell models often display a lower uptake due to stronger barrier function (Artursson and Karlsson, 1991). In contrast, sometimes *in vitro* models show enhanced uptake via micropinocytosis and so lead to an overestimation of cellular uptake (Weissleder et al., 2014). We applied different methods to investigate cellular uptake. The side scatter analysis, as a second method, reflected a much larger highly granular cell fraction with the highest exposure of 100 µg Al/mL for 24 h, as compared to only 5% in intestinal Caco-2 cells in the previous study (Sieg et al., 2018). This leads to the assumption that liver cells are more prone to Al nanoparticle uptake than intestinal cells. Similar to what was observed with intestinal cells in previous studies, the cellular uptake of ionic species was less than the particle uptake. This has been described before as the “Trojan horse effect” (Hsiao et al., 2015, Semisch et al., 2014). While ionic Al uptake into HepG2 turned out to be almost negligible, a fraction of up to 10 % of the administered ionic Al was taken up by HepaRG, or showed at least a strong interaction with the cell monolayer which was not removable during the washing procedure. This could be caused by the morphological structure of hepatocytes , simulated bile-canaliculi-like structures and biliary epithelial-like cells (Guillouzo et al., 2007) which are closer to the *in vivo* situation which is highly accessible to any material which is coming from the bloodstream through fenestrated liver sinusoids. HepG2 cells tend to form smaller cell clusters of undifferentiated cells which enlarge the area of contact of cell membranes with the Al-containing medium. For this reason, although equal Al concentrations were used, the cellular exposure nevertheless led to comparable results. Remarkably, nanoparticle uptake did not differ significantly between both cell lines.

Al has been described to be related to cellular disorders and diseases (ATSDR, 2008). The underlying mechanisms of action are still disputed, but there is evidence that Al competes

with other metal cations and cofactors and thus disturbs metal ion homeostasis (Macdonald and Martin, 1988). Additionally, Al binds to proteins and blood components (Ganrot, 1986). In hepatic cell lines, Al toxicity occurs at lower concentrations, as compared to intestinal cells (Sieg et al., 2018). Hepatic cells *in vivo* are much less exposed to Al after oral uptake, compared to intestinal cells. The intestinal barrier thus shields other tissues to orally ingested Al. Our finding that Al nanoparticles are taken up in a higher amount than dissolved ionic Al might possibly induce an additional hazardous potential of particulate Al. *In vitro* toxicity of $AlCl_3$ to liver cells was shown before (Mailloux and Appanna, 2007) and some *in vivo* studies showed effects of Al on the liver of chicken (Wang et al., 2016), piglets (Alemmari et al., 2011), and rats (Zhu et al., 2013). However, specific nanoparticulate effects are still disputed. While some studies underline nano-specific effects of Al_2O_3 nanoparticles (Chen et al., 2008, Oesterling et al., 2008, Zhang et al., 2011), others negate this hypothesis (Radziun et al., 2011, Sun et al., 2011). Effects of elementary Al nanoparticles were investigated in the present study on liver cells for the first time. Our results demonstrate that cellular uptake of Al is increased when applied in nano-form, but at the same time they support the assumption that there is no nano-specific toxicity caused by Al-containing nanoparticles in the liver cell lines HepG2 and HepaRG, although cellular uptake of these substances is elevated in the nano form. Nanoparticulate Al appears to deposit Al in or on the cells without an additional impact on the outcome of short-term *in vitro* toxicity testing.

There are several mechanistic hypotheses in literature to explain the mode(s) of action of Al toxicity. It is described to be a result of oxidative damage and disturbed metal ion homeostasis (Han et al., 2013). In detail, the authors suggest that the initiating step is the ability of Al to replace functional metal ions such as iron, calcium or magnesium. This can alter protein function and lead to an excess of free iron in the cells. Another direct interaction is the binding of phosphate groups, which can be part of the cell membrane, the DNA or nucleoside triphosphates (Tomljenovic, 2011). Metabolic enzymes, like those of the cytochrome P450 family, can be affected as well (Bidlack et al., 1987). An oxidative environment is created which has a negative impact on cellular functions (Mailloux et al., 2011, Gonzalez et al., 2007, Yousef, 2004). Targets of this oxidative stress are nucleic acids, proteins, lipids, and the whole mitochondria. Lipid peroxidation provokes a decrease in membrane fluidity and the excess of ROS formation disturbs and multiple regulatory and signaling functions (Han et al., 2013). At the cellular level, these factors lead to a loss of mitochondrial function (Levi and Rovida, 2009). We confirmed such effects as reduced GSH levels in HepG2 cells and disturbed mitochondrial membrane potential in HepaRG cells treated with ionic $AlCl_3$. Furthermore, an induction of pro-apoptotic genes in human brain cells by Al has been reported (Lukiw et al., 2005). The results of the present study show

induction of apoptosis by ionic Al in hepatic cells as well. At the same time, there is no evidence for a nano-specific hazard of Al, since no effects were caused by the investigated nanoparticulate Al species. Nevertheless, effects over a longer time period, that result from "trojan-horse"-like uptake and slow dissolution and accumulation inside the cells cannot be excluded to cause hazard. There is evidence for genotoxic effects of Al in rats *in vivo* (Geyikoglu et al., 2013, Turkez et al., 2010). However, most *in vitro* cell systems yielded negative results in standard genotoxicity measurements (Krewski et al., 2007). Nevertheless, there are indications for chromosomal damage caused by Al (Kumar et al., 2009). Therefore, it must be taken into account that genotoxicity can be an indirect result of oxidative damage (Abubakar et al., 2003, Turkez et al., 2013) and cytotoxicity (Galloway, 2000).

Although Al toxicity has been discussed over decades, its toxicological potential has gained more public attention (Klein, 2005), with a focus on the different Al-species-specific effects of soluble ions and nanoparticles. Recently, the balance between nanoparticles and ionic compounds is more and more described as a dynamic situation which depends on particle solubility and the formation of different soluble ionic species in a complex mixture. The cellular mode(s) of action are still being disputed among researchers. Due to its ubiquitous presence, a daily chronic oral uptake of Al is unavoidable (Klotz et al., 2017). Conversions between different particulate and dissolved species occur in the gastrointestinal tract (Sieg et al., 2017). Hence, there is a potential concern of an increased nano-specific hazard caused by ingested Al-containing particles. This study contributes comprehensive information that Al uptake occurs preferably in particulate form, while cellular effects are mainly caused by high concentrations of ionic Al. An increased toxicological hazard caused by nanoparticles was not detected.

Conclusion

Aluminum is frequently ingested by humans and is systemically distributed in the human body, including the liver. It occurs in various partially convertible chemical species which show differences in solubility and particle formation. In this study, elementary Al^0 nanoparticles, γ-Al_2O_3 nanoparticles and the soluble species $AlCl_3$ were investigated. Each of these species can, amongst others, enter the liver and lead to species-specific cellular effects. Cellular uptake into HepG2 and HepaRG cells was investigated by optical and electron microscopy, element- and side scatter analysis. It was shown that particulate Al is preferentially taken up into both cell lines. Inversely, soluble Al showed increased toxic effects while the two particle species did not. Cellular endpoints, such as cell viability, cellular impedance, cell death, oxidative stress, mitochondrial membrane potential and DNA damage were investigated. No increased acute toxicity of nanoparticles compared to initially ionic Al species was detectable. High concentrations of ionic Al above 100 µg Al/mL caused effects on a variety of investigated endpoints, while particulate Al did not. While liver cells were only slightly affected by $AlCl_3$ after short-term exposure, nevertheless, since Al tends to accumulate in the liver over the human lifetime, impairment of liver functions following a long-term-exposure to Al cannot be excluded.

Declaration of interest

The authors declare no conflict of interest.

Acknowledgements

This publication, as part of the German-French SolNanoTOX project was funded by the German Research Foundation DFG (Grant Number LA 3411/1-1) and by the French "Agence Nationale de la Recherche" ANR (Project ID ANR-13-IS10-0005). We thank the BfR Department of Chemical and Product Safety and the German Institute for Materials Research and Testing for material supply and particle characterization.

Supplementary Information

Supplementary Table 1: Particle characterization parameters. The particle characterization of the applied nanoparticles was already published (Sieg et al., 2017, Krause et al., 2018) and is summed up in this table. CCM: Cell culture medium (DMEM + 10% FCS + 1% Pen/Strep) as described in the methods chapter. Results did not differ significantly in both used cell culture media.

Parameter	Al^0 NP	Al_2O_3 NP	Method	Published source
Particle shape	spheric	elongated	TEM	(Sieg et al., 2017)
Core Radii	> 5 nm	2.5 x 15 nm	TEM	(Sieg et al., 2017)
Core Radii	> 8 nm	5 - 10 nm	SAXS	(Sieg et al., 2017)
Hydrodynamic Diameter in stock dispersion	250 – 270 nm	170 – 210 nm	DLS	(Krause et al., 2018)
Hydrodynamic Diameter in CCM	200 – 220 nm	70 – 230 nm	DLS	(Krause et al., 2018)
Oxidation state	elementary with oxidized surface layer	entirely oxidized	TEM / XRD	(Krause et al., 2018)
Initial free ionic amount	0.01 %	0.02 %	AAS	(Sieg et al., 2017)
Ion release in CCM	0.9 % in 48 h	0.5 % in 48 h	AAS	(Sieg et al., 2018)
Trace element composition in stock dispersion	P > Cl > S > K > Ca	Cl > S > P > K > Ca	IBM	(Sieg et al., 2017)

Supplementary Table 2: Sample Volumes, applied concentrations for each experiments and culture areas. All concentrations were calculated based on the aluminum amount in µg Al / mL. *For cell viability screening a range of 4 - 200 µg Al / mL was applied. For further cellular assays, 4, 25 and 100 µg Al / mL were used.

Format	Sample volume mL	Volume concentration µg Al / mL	Well area cm²	Concentration µg Al / cm²	Total Al mass µg	Experimental Application
96-well	0.1	4	0.33	1.33	0.4	Cell Viability*, Cellular Impedance, Oxidative Stress Measurements, High-Content Analysis (HepG2 and HepaRG) and Flow Cytometry (HepaRG)
	0.1	10	0.33	3.33	1	
	0.1	25	0.33	8.33	2.5	
	0.1	50	0.33	16.67	5	
	0.1	100	0.33	33.33	10	
	0.1	150	0.33	50	15	
	0.1	200	0.33	66.67	20	
12-well	1	4	3.8	1.05	4	Flow Cytometry (HepG2)
	1	25	3.8	6.58	25	
	1	100	3.8	26.32	100	
	1	50	3.8	13.16	50	Element Analysis (HepG2 and HepaRG)

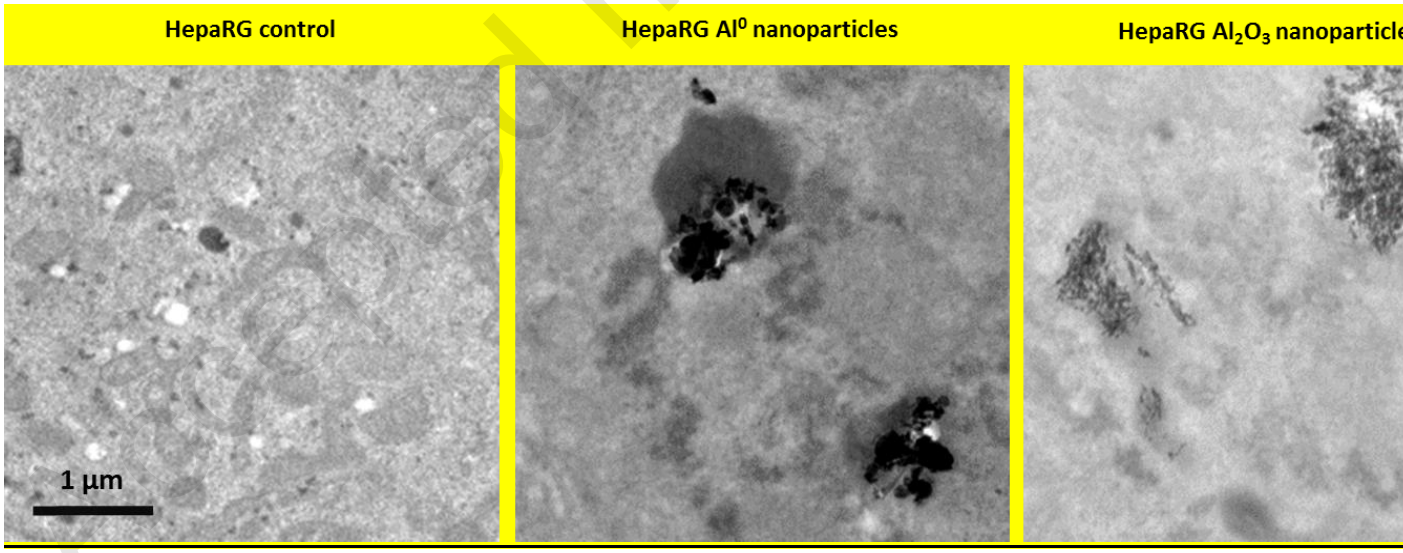

Supplementary Figure 1: Enlarged areas of TEM pictures as shown in Figure 1. Al and Al_2O_3 nanoparticle uptake can be seen by electron microscopy.

References

ABDEL-WAHAB, W. M. 2012. AlCl3-Induced Toxicity and Oxidative Stress in Liver of Male Rats: Protection by Melatonin *Life Science Journal-Acta, Zhengzhou University Overseas Edition, 9(4): p. 1173-1182*.

ABUBAKAR, M. G., TAYLOR, A. & FERNS, G. A. 2003. Aluminium administration is associated with enhanced hepatic oxidant stress that may be offset by dietary vitamin E in the rat. *Int J Exp Pathol,* 84**,** 49-54.

ALEMMARI, A., MILLER, G. G., ARNOLD, C. J. & ZELLO, G. A. 2011. Parenteral aluminum induces liver injury in a newborn piglet model. *J Pediatr Surg,* 46**,** 883-7.

ALFREY, A. C., HEGG, A. & CRASWELL, P. 1980. Metabolism and toxicity of aluminum in renal failure. *Am J Clin Nutr,* 33**,** 1509-16.

ALFREY, A. C., LEGENDRE, G. R. & KAEHYNE, W. D. 1976. The dialysis encephalopathy syndrome. Possible aluminium intoxication. *New Engl J Med,* 294.

ANINAT, C., PITON, A., GLAISE, D., LE CHARPENTIER, T., LANGOUET, S., MOREL, F., GUGUEN-GUILLOUZO, C. & GUILLOUZO, A. 2006. Expression of cytochromes P450, conjugating enzymes and nuclear receptors in human hepatoma HepaRG cells. *Drug Metab Dispos,* 34**,** 75-83.

ANTHERIEU, S., CHESNE, C., LI, R., CAMUS, S., LAHOZ, A., PICAZO, L., TURPEINEN, M., TOLONEN, A., UUSITALO, J., GUGUEN-GUILLOUZO, C. & GUILLOUZO, A. 2010. Stable expression, activity, and inducibility of cytochromes P450 in differentiated HepaRG cells. *Drug Metab Dispos,* 38**,** 516-25.

ARTURSSON, P. & KARLSSON, J. 1991. Correlation between oral drug absorption in humans and apparent drug permeability coefficients in human intestinal epithelial (Caco-2) cells. *Biochem Biophys Res Commun,* 175**,** 880-5.

ATSDR 2008. (Agency for Toxic Substances and Disease Registry), Toxicological Profile for Aluminum. Atlanta: U.S. Department of

Health and Human Services, Public Health Service. pp. 357.

BIDLACK, W. R., BROWN, R. C., MESKIN, M. S., LEE, T. C. & KLEIN, G. L. 1987. Effect of aluminum on the hepatic mixed function oxidase and drug metabolism. *Drug Nutr Interact,* 5**,** 33-42.

CAROLI, S., ALIMONTI, A., CONI, E., PETRUCCI, F., SENOFONTE, O. & VIOLANTE, N. 1994. The Assessment of Reference Values for Elements in Human Biological Tissues and Fluids: A Systematic Review. *Critical Reviews in Analytical Chemistry,* 24**,** 363-398.

CHEN, L., YOKEL, R. A., HENNIG, B. & TOBOREK, M. 2008. Manufactured aluminum oxide nanoparticles decrease expression of tight junction proteins in brain vasculature. *J Neuroimmune Pharmacol,* 3**,** 286-95.

CUNAT, L., LANHERS, M. C., JOYEUX, M. & BURNEL, D. 2000. Bioavailability and intestinalabsorption of aluminum in rats: effects of aluminum compounds and some dietary constituents. *Biol Trace Elem Res,* 76.

DARBRE, P. D. 2009. Underarm antiperspirants/deodorants and breast cancer. *Breast Cancer Res,* 11 Suppl 3**,** S5.

ECHEGOYEN, Y., RODRIGUEZ, S. & NERIN, C. 2016. Nanoclay migration from food packaging materials. *Food Addit Contam Part A Chem Anal Control Expo Risk Assess,* 33**,** 530-9.

EMSLEY, J. 1991. *The elements,* Oxford, Clarendon Press.

EXLEY, C. 2003. A biogeochemical cycle for aluminium? *J Inorg Biochem,* 97**,** 1-7.

GALLOWAY, S. M. 2000. Cytotoxicity and chromosome aberrations in vitro: experience in industry and the case for an upper limit on toxicity in the aberration assay. *Environ Mol Mutagen,* 35**,** 191-201.

GANROT, P. O. 1986. Metabolism and possible health effects of aluminum. *Environ Health Perspect,* 65**,** 363-441.

GERETS, H. H., TILMANT, K., GERIN, B., CHANTEUX, H., DEPELCHIN, B. O., DHALLUIN, S. & ATIENZAR, F. A. 2012. Characterization of primary human hepatocytes, HepG2 cells, and HepaRG cells at the mRNA level and CYP activity in response to inducers and their predictivity for the detection of human hepatotoxins. *Cell Biol Toxicol,* 28**,** 69-87.

GEYIKOGLU, F., TURKEZ, H., BAKIR, T. O. & CICEK, M. 2013. The genotoxic, hepatotoxic, nephrotoxic, haematotoxic and histopathological effects in rats after aluminium chronic intoxication. *Toxicol Ind Health,* 29**,** 780-91.

GHORBEL, I., CHAABANE, M., ELWEJ, A., BOUDAWARA, O., ABDELHEDI, S., JAMOUSSI, K., BOUDAWARA, T. & ZEGHAL, N. 2016. Expression of metallothioneins I and II related to oxidative stress in the liver of aluminium-treated rats. *Arch Physiol Biochem,* 122**,** 214-222.

GONZALEZ, M. A., ALVAREZ MDEL, L., PISANI, G. B., BERNAL, C. A., ROMA, M. G. & CARRILLO, M. C. 2007. Involvement of oxidative stress in the impairment in biliary secretory function induced by intraperitoneal administration of aluminum to rats. *Biol Trace Elem Res,* 116**,** 329-48.

GUILLOUZO, A., CORLU, A., ANINAT, C., GLAISE, D., MOREL, F. & GUGUEN-GUILLOUZO, C. 2007. The human hepatoma HepaRG cells: a highly differentiated model for studies of liver metabolism and toxicity of xenobiotics. *Chem Biol Interact,* 168**,** 66-73.

HAN, S., LEMIRE, J., APPANNA, V. P., AUGER, C., CASTONGUAY, Z. & APPANNA, V. D. 2013. How aluminum, an intracellular ROS generator promotes hepatic and neurological diseases: the metabolic tale. *Cell Biol Toxicol,* 29**,** 75-84.

HSIAO, I. L., HSIEH, Y. K., WANG, C. F., CHEN, I. C. & HUANG, Y. J. 2015. Trojan-horse mechanism in the cellular uptake of silver nanoparticles verified by direct intra- and extracellular silver speciation analysis. *Environ Sci Technol,* 49**,** 3813-21.

KAMENCIC, H., LYON, A., PATERSON, P. G. & JUURLINK, B. H. 2000. Monochlorobimane fluorometric method to measure tissue glutathione. *Anal Biochem,* 286**,** 35-7.

KEITH, L. S., JONES, D. E. & CHOU, C. H. 2002. Aluminum toxicokinetics regarding infant diet and vaccinations. *Vaccine,* 20 Suppl 3**,** S13-7.

KLEIN, G. L. 2005. Aluminum: new recognition of an old problem. *Curr Opin Pharmacol,* 5**,** 637-40.

KLOTZ, K., WEISTENHOFER, W., NEFF, F., HARTWIG, A., VAN THRIEL, C. & DREXLER, H. 2017. The Health Effects of Aluminum Exposure. *Dtsch Arztebl Int,* 114**,** 653-659.

KRAUSE, B., MEYER, T., SIEG, H., KASTNER, C., REICHARDT, P., TENTSCHERT, J., JUNGNICKEL, H., ESTRELA-LOPIS, I., BUREL, A., CHEVANCE, S., GAUFFRE, F., JALILI, P., MEIJER, J., BOHMERT, L., BRAEUNING, A., THUNEMANN, A. F., EMMERLING, F., FESSARD, V., LAUX, P., LAMPEN, A. & LUCH, A. 2018. Characterization of aluminum, aluminum oxide and titanium dioxide nanomaterials using a combination of methods for particle surface and size analysis. *RSC Advances,* 8**,** 14377-14388.

KREWSKI, D., YOKEL, R. A., NIEBOER, E., BORCHELT, D., COHEN, J., HARRY, J., KACEW, S., LINDSAY, J., MAHFOUZ, A. M. & RONDEAU, V. 2007. Human health risk assessment for aluminium, aluminium oxide, and aluminium hydroxide. *J Toxicol Environ Health B Crit Rev,* 10 Suppl 1**,** 1-269.

KUMAR, V., BAL, A. & GILL, K. D. 2009. Aluminium-induced oxidative DNA damage recognition and cell-cycle disruption in different regions of rat brain. *Toxicology,* 264**,** 137-44.

LEVI, S. & ROVIDA, E. 2009. The role of iron in mitochondrial function. *Biochim Biophys Acta,* 1790**,** 629-36.

LICHTENSTEIN, D., EBMEYER, J., MEYER, T., BEHR, A. C., KASTNER, C., BOHMERT, L., JULING, S., NIEMANN, B., FAHRENSON, C., SELVE, S., THUNEMANN, A. F., MEIJER, J., ESTRELA-LOPIS, I., BRAEUNING, A. & LAMPEN, A. 2016. It takes more than a coating to get nanoparticles through the intestinal barrier in vitro. *Eur J Pharm Biopharm*.

LIDSKY, T. I. 2014. Is the Aluminum Hypothesis Dead? *Journal of Occupational and Environmental Medicine,* 56**,** S73-S79.

LIN, C. Y., HSIAO, W. C., HUANG, C. J., KAO, C. F. & HSU, G. S. 2013. Heme oxygenase-1 induction by the ROS-JNK pathway plays a role in aluminum-induced anemia. *J Inorg Biochem,* 128**,** 221-8.

LOTE, C. J. & SAUNDERS, H. 1991. Aluminium: gastrointestinal absorption and renal excretion. *Clin Sci (Lond),* 81**,** 289-95.
LUCKERT, C., SCHULZ, C., LEHMANN, N., THOMAS, M., HOFMANN, U., HAMMAD, S., HENGSTLER, J. G., BRAEUNING, A., LAMPEN, A. & HESSEL, S. 2017. Comparative analysis of 3D culture methods on human HepG2 cells. *Archives of Toxicology,* 91**,** 393-406.
LUKIW, W. J., PERCY, M. E. & KRUCK, T. P. 2005. Nanomolar aluminum induces pro-inflammatory and pro-apoptotic gene expression in human brain cells in primary culture. *J Inorg Biochem,* 99**,** 1895-8.
MACDONALD, T. L. & MARTIN, R. B. 1988. Aluminum ion in biological systems. *Trends Biochem Sci,* 13**,** 15-9.
MAILLOUX, R. J. & APPANNA, V. D. 2007. Aluminum toxicity triggers the nuclear translocation of HIF-1alpha and promotes anaerobiosis in hepatocytes. *Toxicol In Vitro,* 21**,** 16-24.
MAILLOUX, R. J., LEMIRE, J. & APPANNA, V. D. 2011. Hepatic response to aluminum toxicity: dyslipidemia and liver diseases. *Exp Cell Res,* 317**,** 2231-8.
NIEBOER, E., GIBSON, B. L., OXMAN, A. D. & KRAMER, J. R. 1995. Health effects of aluminum: a critical review with emphasis on aluminum in drinking water. *Environmental Reviews,* 3**,** 29-81.
OESTERLING, E., CHOPRA, N., GAVALAS, V., ARZUAGA, X., LIM, E. J., SULTANA, R., BUTTERFIELD, D. A., BACHAS, L. & HENNIG, B. 2008. Alumina nanoparticles induce expression of endothelial cell adhesion molecules. *Toxicol Lett,* 178**,** 160-6.
RADZIUN, E., DUDKIEWICZ WILCZYNSKA, J., KSIAZEK, I., NOWAK, K., ANUSZEWSKA, E. L., KUNICKI, A., OLSZYNA, A. & ZABKOWSKI, T. 2011. Assessment of the cytotoxicity of aluminium oxide nanoparticles on selected mammalian cells. *Toxicol In Vitro,* 25**,** 1694-700.
REPETTO, G., DEL PESO, A. & ZURITA, J. L. 2008. Neutral red uptake assay for the estimation of cell viability/cytotoxicity. *Nat Protoc,* 3**,** 1125-31.
SCHINTU, M., MELONI, P. & CONTU, A. 2000. Aluminum fractions in drinking water from reservoirs. *Ecotoxicol Environ Saf,* 46**,** 29-33.
SCHÖNHOLZER, K. W., SUTTON, R. A., WALKER, V. R., SOSSI, V., SCHULZER, M., ORVIG, C., VENCZEL, E., JOHNSON, R. R., VETTERLI, D., DITTRICH-HANNEN, B., KUBIK, P. & SUTER, M. 1997. Intestinal absorption of trace amounts of aluminium in rats studied with 26aluminium and accelerator mass spectrometry. *Clin Sci (Lond),* 92**,** 379-83.
SEMISCH, A., OHLE, J., WITT, B. & HARTWIG, A. 2014. Cytotoxicity and genotoxicity of nano - and microparticulate copper oxide: role of solubility and intracellular bioavailability. *Part Fibre Toxicol,* 11**,** 10.
SIEG, H., BRAEUNING, C., KUNZ, B. M., DAHER, H., KASTNER, C., KRAUSE, B. C., MEYER, T., JALILI, P., HOGEVEEN, K., BOHMERT, L., LICHTENSTEIN, D., BUREL, A., CHEVANCE, S., JUNGNICKEL, H., TENTSCHERT, J., LAUX, P., BRAEUNING, A., GAUFFRE, F., FESSARD, V., MEIJER, J., ESTRELA-LOPIS, I., THUNEMANN, A. F., LUCH, A. & LAMPEN, A. 2018. Uptake and molecular impact of aluminum-containing nanomaterials on human intestinal caco-2 cells. *Nanotoxicology***,** 1-22.
SIEG, H., KÄSTNER, C., KRAUSE, B., MEYER, T., BUREL, A., BÖHMERT, L., LICHTENSTEIN, D., JUNGNICKEL, H., TENTSCHERT, J., LAUX, P., BRAEUNING, A., ESTRELA-LOPIS, I., GAUFFRE, F., FESSARD, V., MEIJER, J., LUCH, A., THÜNEMANN, A. F. & LAMPEN, A. 2017. Impact of an Artificial Digestion Procedure on Aluminum-Containing Nanomaterials. *Langmuir,* 33**,** 10726-10735.
STAHL, T., TASCHAN, H. & BRUNN, H. 2011. Aluminium content of selected foods and food products. *Environmental Sciences Europe,* 23**,** 37.
SUN, J., WANG, S., ZHAO, D., HUN, F. H., WENG, L. & LIU, H. 2011. Cytotoxicity, permeability, and inflammation of metal oxide nanoparticles in human cardiac microvascular endothelial cells: cytotoxicity, permeability, and inflammation of metal oxide nanoparticles. *Cell Biol Toxicol,* 27**,** 333-42.

SWEGERT, C. V., DAVE, K. R. & KATYARE, S. S. 1999. Effect of aluminium-induced Alzheimer like condition on oxidative energy metabolism in rat liver, brain and heart mitochondria. *Mech Ageing Dev,* 112**,** 27-42.
TOMLJENOVIC, L. 2011. Aluminum and Alzheimer's disease: after a century of controversy, is there a plausible link? *J Alzheimers Dis,* 23**,** 567-98.
TURKEZ, H., GEYIKOGLU, F. & TATAR, A. 2013. Borax counteracts genotoxicity of aluminum in rat liver. *Toxicol Ind Health,* 29**,** 775-9.
TURKEZ, H., YOUSEF, M. I. & GEYIKOGLU, F. 2010. Propolis prevents aluminium-induced genetic and hepatic damages in rat liver. *Food Chem Toxicol,* 48**,** 2741-6.
VAN OOSTDAM, J. C., ZWANENBURG, H. & HARRISON, J. R. 1990. Canadian perspectives on aluminum. *Environ Geochem Health,* 12**,** 71-4.
VICK, K. E. & JOHNSON, C. A. 1985. Aluminum-related osteomalacia in renal-failure patients. *Clin Pharm,* 4**,** 434-9.
WAGNER, W. 1999. *Canadian Minerals Yearbook. Ottawa: Natural Resources Canada*.
WALTON, J. R. 2014. Chronic aluminum intake causes Alzheimer's disease: applying Sir Austin Bradford Hill's causality criteria. *J Alzheimers Dis,* 40**,** 765-838.
WANG, B., ZHU, Y., ZHANG, H., LIU, L., LI, G., SONG, Y. & LI, Y. 2016. Effects of aluminum chloride on serum proteins, bilirubin, and hepatic trace elements in chickens. *Toxicol Ind Health,* 32**,** 1693-9.
WEISSLEDER, R., NAHRENDORF, M. & PITTET, M. J. 2014. Imaging macrophages with nanoparticles. *Nat Mater,* 13**,** 125-38.
WILLHITE, C. C., BALL, G. L. & MCLELLAN, C. J. 2012. Total allowable concentrations of monomeric inorganic aluminum and hydrated aluminum silicates in drinking water. *Crit Rev Toxicol,* 42**,** 358-442.
WILLHITE, C. C., KARYAKINA, N. A., YOKEL, R. A., YENUGADHATI, N., WISNIEWSKI, T. M., ARNOLD, I. M., MOMOLI, F. & KREWSKI, D. 2014. Systematic review of potential health risks posed by pharmaceutical, occupational and consumer exposures to metallic and nanoscale aluminum, aluminum oxides, aluminum hydroxide and its soluble salts. *Crit Rev Toxicol,* 44 Suppl 4**,** 1-80.
XU, F., LIU, Y., ZHAO, H., YU, K., SONG, M., ZHU, Y. & LI, Y. 2017. Aluminum chloride caused liver dysfunction and mitochondrial energy metabolism disorder in rat. *J Inorg Biochem,* 174**,** 55-62.
YOKEL, R. A., URBAS, A. A., LODDER, R. A., SELEGUE, J. P. & FLORENCE, R. L. 2005. 26Al-containing acidic and basic sodium aluminum phosphate preparation and use in studies of oral aluminum bioavailability from foods utilizing 26Al as an aluminum tracer. *Nuclear Instruments and Methods in Physics Research Section B: Beam Interactions with Materials and Atoms,* 229**,** 471-478.
YOUSEF, M. I. 2004. Aluminium-induced changes in hemato-biochemical parameters, lipid peroxidation and enzyme activities of male rabbits: protective role of ascorbic acid. *Toxicology,* 199**,** 47-57.
YUAN, C. Y., LEE, Y. J. & HSU, G. S. 2012. Aluminum overload increases oxidative stress in four functional brain areas of neonatal rats. *J Biomed Sci,* 19**,** 51.
ZATTA, P., KISS, T., SUWALSKY, M. & BERTHON, G. 2002. Aluminium(III) as a promoter of cellular oxidation. *Coordination Chemistry Reviews,* 228**,** 271-284.
ZHANG, X. Q., YIN, L. H., TANG, M. & PU, Y. P. 2011. ZnO, TiO(2), SiO(2,) and Al(2)O(3) nanoparticles-induced toxic effects on human fetal lung fibroblasts. *Biomed Environ Sci,* 24**,** 661-9.
ZHU, Y., HAN, Y., ZHAO, H., LI, J., HU, C., LI, Y. & ZHANG, Z. 2013. Suppressive effect of accumulated aluminum trichloride on the hepatic microsomal cytochrome P450 enzyme system in rats. *Food Chem Toxicol,* 51**,** 210-4.